

# Acousto-Ultrasonic Structural Health Monitoring of Aerospace Composite Materials

# Acousto-Ultrasonic Structural Health Monitoring of Aerospace Composite Materials

M. Gresil
*School of materials, University of Manchester, UK*
A. Muller & C. Soutis
*Aerospace Research Institute, University of Manchester, UK*

ABSTRACT: Piezoelectric transducers have a long history of applications in nondestructive evaluation (NDE) of material and structure integrity owing to their ability of transforming mechanical energy to electrical energy and vice versa. From an acoustic point of view, there is no difference between structural health monitoring (SHM) and conventional NDE since both rely on the same physics in the sense that in either case acoustic waves are generated and then detected. SHM was 'born' from the conjunction of several techniques and has a common basis with NDE. In fact, several NDE techniques can be converted into SHM techniques, by integrating sensors and actuators inside the monitored structure. For instance, traditional ultrasonic testing can be easily converted into an acousto-ultrasonic SHM system, using embedded or surface-mounted piezoelectric wafer active sensors (PWAS). These sensors should be affordable, lightweight, and unobtrusive such as to not impose cost and weight penalty on the structure and to not interfere with the structural strength and airworthiness. Other damage measuring methods based on large area measurements have been used in SHM development for verification and validation of damage and/or for understating the proposed SHM approach; however, they do not seem appropriate for permanent installation onto the monitored structure and will not be discussed under the heading of 'SHM sensors'. This paper presents and discusses an overview of ultrasonic SHM techniques for composite materials. After a brief introduction, it presents the PWAS-based SHM principle, which is followed by a discussion of the passive and active ultrasonic SHM techniques. The paper identifies advantages and disadvantages of these in-situ NDE methods and guidelines for future work on heterogeneous, anisotropic materials, like aerospace composite polymer.

## 1 INTRODUCTION

Structural health monitoring (SHM) was born from the conjunction of several techniques and has a common basis with non-destructive evaluation (NDE). In fact, several NDE techniques can be converted into SHM techniques, by integrating sensors and actuators inside the monitored structure. For instance, traditional ultrasonic testing can be easily converted into an acousto-ultrasonic SHM system, using embedded or surface-mounted piezoelectric wafer active sensors (PWAS). These sensors should be affordable, lightweight, and unobtrusive such as to not impose cost and weight penalty on the structure and to not interfere with the structural strength and airworthiness.

Other damage measuring methods based on large area measurements (ultrasonic C-scans, thermography, etc.) have been used in SHM development for verification and validation of damage and/or for understating the proposed SHM approach; however, they do not seem appropriate for permanent installation onto the monitored structure and will not be discussed in this paper.

This paper presents a brief overview of acousto-ultrasonic SHM techniques and discusses the PWAS-based SHM principle of aerospace composite materials. It follows with a discussion of the passive and the active acousto-ultrasonic SHM techniques. The paper ends with a conclusion and guidelines for future work.

### 1.1 *Background*

The end of the twentieth century has brought new problematic to the aeronautical industry and research. On the one hand, the air transport has given rise to an exponential growth of passenger in air traffic, resulting in an increased demand. On the other hand, a global objective such as the reduction of the impact on environment has to be considered. Therefore, major modern challenges for aeronautical research are to reconcile the improvement of aircraft efficiency, the economical aspect (ie: manufacturing, fuel, and maintenance cost) and the extension of operational lifetime without compromising the aircraft safety and reliability (ACARE, 2001; Pfeiffer & Wevers, 2007). In consideration of those challenges, the European Commission has published in 2001 a report titled "European Aeronautics: a vision for 2020" describing the research objectives and expected advancement of the aeronautical research for 2020 (ACARE, 2001).

Over the past 30 years composite materials have been increasingly used in aircraft structures (Diamanti & Soutis, 2010; Grondel, Assaad, Delebarre, & Moulin, 2004; Staszewski, Mahzan, & Traynor, 2009). Recent designed aircraft such as the Airbus A380 introduced in 2007 and the Boeing B787 introduced in 2011 have their structures made of 25% and 50% of composite materials respectively (Staszewski et al., 2009). This growing interest for composite materials in aviation over aluminium alloys is mainly due to their excellent specific properties such as high stiffness and strength for weight ratio (especially in case of polymer matrix composite). The particular properties of composite materials offer new design perspective. For instance their anisotropic properties can be tailored to design requirements and improve the aerodynamic while using lighter components. This, on a larger scale, can impact aircraft efficiency and therefore, contribute to the achievement of current research objectives.

### 1.2 *Common damages in aircraft composite structure*

Many researchers agreed that impact damage is one of the most frequent damage encountered by aircraft structure (Diamanti & Soutis, 2010; Grondel et al., 2004; Haase, Thomson, Bishop, & Isambert, 2013; Staszewski et al., 2009) . A major concern is that some impact damages in composite materials do not provide visible evidence, therefore may not be detected during regular surface inspection. Those particular damages are known as BVID (Barely Visible Impact Damage) and concern principally two type of impact damages: the low velocity (and low energy) impact damages, which are associated with a velocity ranging between 4 to 8 $m.s^{-1}$ and an impact energy up to 50 J; and the high energy low velocity impact damages (Haase et al., 2013). Most of the incidents generating BVID occur during ground operations, common examples include: bird strikes, runway debris, tool drops during maintenance, or collision with ground vehicles (Grondel et al., 2004; Haase et al., 2013). In addition to BVID, Grondel (2004) identified debondings are another common type of hidden damages difficult to detect with visual inspection.

Those damages or defects often initiate further damages, such as matrix crack growth, delamination, or fibres breakage. Therefore, they are the starting point to reduction of the composites strength and degradation of its structural integrity (Grondel et al., 2004; Staszewski et al., 2009). Failure to detect damage before it expands and reach a critical size may lead to failure of the component. A late damage detection can result in extra cost due for instance to replacement but also to aircraft service interruption. Moreover, the cost of repair and maintenance represent a quarter of the expense for commercial aircraft in-service (Giurgiutiu, 2008). For instance, in 2000 the cost by the Airports Council International (ACI) related to aircraft collision with ground vehicle was estimated to $3 billion (Haase et al., 2013). In the worst-case scenario such situation may lead to catastrophic failure of the aircraft and jeopardize users safety. In consequence, the detection of those damages as well as other flaws or defect is crucial. On the one hand to allow detection of the damaged area before it reaches a critical size, hence to ensure structure integrity and overall aircraft safety, on the other hand to provide sufficient time for action, such as by monitoring or preventing further growth of the damage (Staszewski et al., 2009).

Therefore, current research focuses on the development or the improvement of NDE for damages detection (especially BVID or other hidden defects) in composite structure. In particular Structural Health Monitoring (SHM) systems have gained growing interest for the development of smart or self-sensing composite structures, leading to a growing amount of literature in field (Diamanti & Soutis, 2010; Giurgiutiu, 2008; Gresil, Soutis, & Giurgiutiu, 2014; Grondel et al., 2004; Ihn & Chang, 2008; Staszewski et al., 2009).

### 1.3 *Piezoelectric wafer active sensors*

Piezoelectric wafer active sensors (Giurgiutiu, 2008) (PWAS) are small, lightweight, and relatively low-cost sensors based on the piezoelectric principle that couples the electrical and mechanical variables in the material (mechanical strain, $S_{ij}$, mechanical stress, $T_{kl}$, electrical field, $E_k$, and electrical displacement $D_j$) in the form:

$$\begin{aligned} S_{ij} &= s^{E}_{ijkl} T_{kl} + d_{kij} E_k \\ D_j &= d_{jkl} T_{kl} + \varepsilon^{T}_{jk} E_k \end{aligned} \quad (1)$$

where $s^{E}_{ijkl}$ is the mechanical compliance of the material measured at zero electric field ($E = 0$), $\varepsilon^{T}_{jk}$ is the dielectric permittivity measured at zero mechanical stress ($T = 0$), and $d_{kij}$ represents the piezoelectric coupling effect. The direct piezoelectric effect converts the stress applied to the sensor into electric charge. Similarly, the converse piezoelectric effect produces strain when a voltage is applied to the sensor.

At ultrasonic frequencies (k-MHz range), PWAS can sense and excite guided Lamb waves traveling long distances along the thin-wall shell structures of aircraft and space vehicles. PWAS are made of thin inexpensive piezo-ceramic wafers electrically poled in the thickness direction and provided with top and bottom electrodes. PWAS can be bonded to the structure with strain-gage installation methodology. They have also been experimentally inserted between the layers of a composite laminate, but this option has raised some structural integrity issues that are still being examined. PWAS have been extensively used for SHM demonstrations because they convert directly electric energy into elastic energy and vice-versa and thus require very simple instrumentation: effective measurements of composite impact waves and guided-waves transmission/reception have been achieved with experimental setups consisting of no more than a signal generator, a digitising oscilloscope, and a PC (Giurgiutiu, 2008).

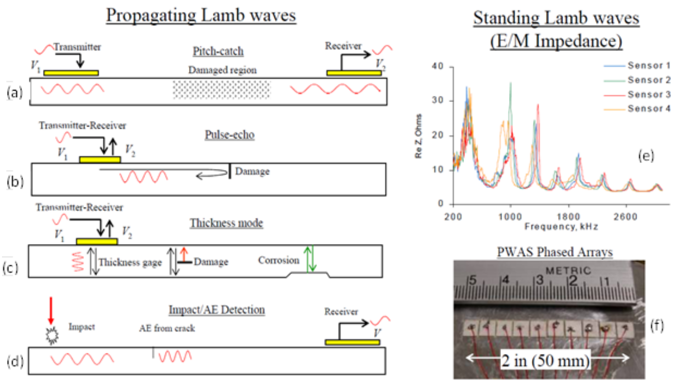


Figure 1. Use of piezoelectric wafer active sensors (PWAS) for damage detection with propagating and standing guided waves in thin-wall structures (Giurgiutiu, 2008).

As shown in Figure 1, PWAS transducers can serve several purposes (Giurgiutiu, 2008): (a) high-bandwidth strain sensors; (b) high-bandwidth wave exciters and receivers; (c) resonators; (d) embedded modal sensors with the electromechanical (E/M) impedance method. By application types, PWAS transducers can be used for (i) **active sensing of far-field damage** using pulse-echo, pitch-catch, and phased-array methods, (ii) **active sensing of near-field damage** using high-frequency E/M impedance method and thickness mode, and (iii) **passive sensing of damage-generating events** through detection of low-velocity impacts and acoustic emission at the tip of advancing cracks. By using Lamb waves in a thin-wall structure, one can detect structural anomaly, i.e., cracks, corrosions, delaminations, and other damage. Because of the physical, mechanical, and piezoelectric properties of PWAS transducers, they act as both transmitters and receivers of Lamb waves travelling through the structure. Figure 1a illustrates the **pitch-catch method**. An electric signal applied at the transmitter PWAS generates, through piezoelectric transduction, elastic waves that travel into the structure and are captured at the receiver PWAS. Figure 1b illustrates the **pulse-echo** method. In this case, the same PWAS transducer acts as both transmitter and receiver. Figure 1c illustrates the use of PWAS transducers in **thickness mode**. The thickness mode is usually excited at much higher frequencies than the guided wave modes discussed in the previous two paragraphs. For example, the thickness mode for a 0.2-mm PWAS is excited at around 11 MHz, whereas the guided wave modes are excited at tens and hundreds of kHz. When operating in thickness mode, the PWAS transducer can act as a thickness gage. Figure 1d illustrates the detection of **impacts and acoustic emission (AE) events**. In this case, the PWAS transducer is operating as a passive receiver of the elastic waves generated by drop weight impacts or by AE events. Figure 1e illustrates the electromechanical impedance spectrum measured in the k-MHz range. When a structure is excited with sustained harmonic excitation of a given frequency, the waves travelling in the structure undergo multiple boundary reflections and settle down in a standing wave pattern know as vibration. Structural vibration is characterised by resonance frequencies at which the structural response goes through peak values. A natural extension of the PWAS pulse-echo method is the development of a PWAS phased array (Figure 1f), which is able to scan a large area from a single location. The PWAS phased arrays utilise the phase array principles to create an interrogating beam of guided waves that travel in a thin-wall structure and can sweep a large area from a single location.

## 2 PASSIVE SHM

This section aims to describe the use of the acoustic emission (AE) technique to contribute to the general problem of SHM and, more generally, to the prediction of the remaining lifetime of industrial materials and structures. AE is primarily used to study the physical parameters and the damage mechanisms of a material, but it is also used as an on-line NDT. The AE phenomenon is based on the release of energy in the form of transitory elastic waves within a material having dynamic deformation processes. The waves, of various types and frequencies, propagate in the material and undergo possible modifications before reaching the surface of the studied sample. A typical source of an AE wave within a material is the appearance of a crack from a defect when the material is put under constraint, or when a pre-existing crack grows. This technique makes it possible to detect in real time the existence of evolutionary defects.

The piezo-based AE sensors are relatively well established in conventional ultrasonic NDE; however, these conventional AE sensors are not quite appropriate for deploying in large numbers on a flight structure due to both cost and size. The SHM sensors (both PWAS and fibre Bragg grating (FBG)) have also been shown capable of AE monitoring: Several authors (Koh, Chiu, Rajic, & Galea, 2003; Martin, Hudd, Wells, Tunnicliffe, & Das-Gupta, 2001; Sung, Oh, Kim, & Hong, 2000) used PWAS, whereas others (Jong-In, Hyung-Joon, Chun-Gon, & Chang-Sun, 2005; Perez, Cui, & Udd, 2001) used FBG sensors for AE emission monitoring. Existing AE monitoring methodology for signal capturing and interpretation (noise filtering, AE events counting algorithms, etc.) can also be used with SHM sensors. PWAS and conventional R15I transducer produced very similar signals (Gresil, Yu, Shen, & Giurgiutiu, 2013). Moreover, using the discrete and the continuous wavelet transform, the AE signal energy is not uniformly distributed between the symmetric and anti-symmetric mode using wavelet transform signal based processing (Gresil et al., 2013).

New concepts, such as distributed sensors and bio-mimetic information acquisition and processing, would also be fundamentally helpful to realise real-time in-situ AE instrumentation for the health monitoring of in-service structures.

## 3 ACTIVE SHM

The AE technique described above makes use of PWAS bonded or embedded in a structure and implemented in a passive way. The same attached sensors can also be used in an active way to produce and detect high-frequency vibrations. A transmitter is used to send a diagnostic stress wave along the structure and a receiver to measure the changes in the received signal caused by the presence of a defect or damage in the structure. This wave propagation approach is a natural extension of traditional NDE techniques, and it is very effective in detecting defects and damage in the form of geometrical discontinuities.

### 3.1 *Guided wave propagation in composites*

The structure under investigation is a CFRP plate consisting of carbon fibre fabric reinforcement in an epoxy resin (Figure 2). The plate dimensions are $390 \times 395 \times 2\,\text{mm}^3$. The CFRP material is HexPly® M18/1/939; this is a woven carbon prepreg manufactured by Hexcel. This material is commonly used in aircraft industry. The plate plies have the orientation $[0, 45, 45, 0]_S$. Twenty one PWAS transducers (Steminc SM412, 8.7 mm-diameter disks and 0.5 mm-thick) were used for Lamb wave propagation experiments. The PWAS network bonded on the CFRP plate is shown on Figure 2. The instrumentation consisted of an HP33120A arbitrary signal generator, and a Tektronix TDS210 digital oscilloscope. A LabView™ computer program was developed to record the data from the digital oscilloscope, and to generate the raw data files.

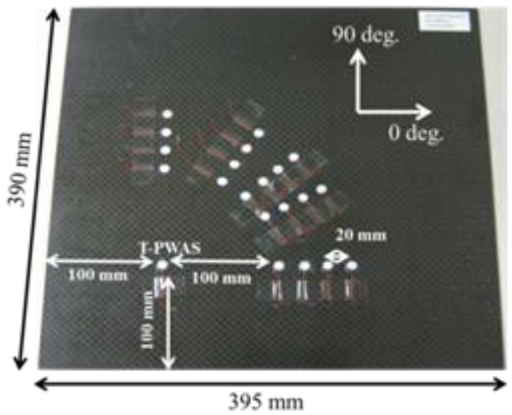


Figure 2. Picture of the network of piezoelectric wafer active sensor bonded on the CFRP.

The multi-physics finite element (MP-FEM) simulation was carried out to determine the attenuation coefficient. A 150 kHz three-tone burst modulated by a Hanning window with a 20 Volts maximum amplitude peak to peak was applied to the top surface of the T-PWAS transducer, and the other PWAS transducers as receivers. Due to the dispersion curves presented and the tuning effect described on reference (Gresil & Giurgiutiu, 2013a; Gresil & Giurgiutiu, 2014), both S0 and A0 modes are present at this frequency. Figure 3 shows the comparison between the MP-FEM simulation and experimental electric signal measured at R-PWAS placed at 100 mm from the T-PWAS with the stiffness proportional coefficient $\beta = 2.10^{-8}$ which corresponds to the A0 mode attenuation as calculated in the reference (Gresil & Giurgiutiu, 2013c; Gresil & Giurgiutiu, 2014). With this stiffness proportional coefficient $\beta = 2.10^{-8}$, the MP-FEM signal for the S0 and the A0 modes are in very good agreement with the experimental signal.

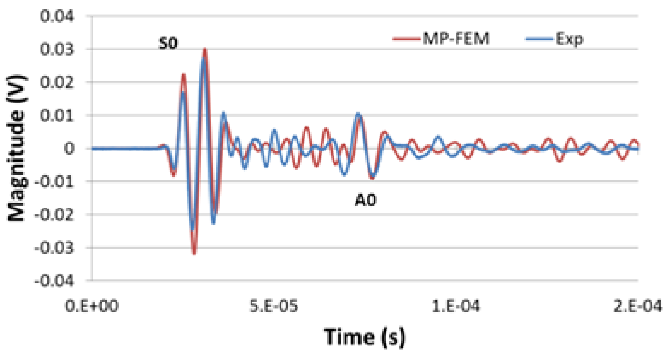


Figure 3. Comparison between the experimental and the MP-FEM received signal at 100 mm from the T-PWAS at 150 kHz with $\alpha = 0$ and $\beta = 2.10^{-8}$ (Gresil & Giurgiutiu 2014).

However, the MP-FEM signal between the S0 mode packet and the A0 mode packet is different from the experimental signal. This different signal may be due to the scattering effect by the other bonded PWAS on the guided wave propagation path between the T-PWAS and the R-PWAS as described on the MP-FEM snapshot on Figure 4 (Gresil & Giurgiutiu, 2014).

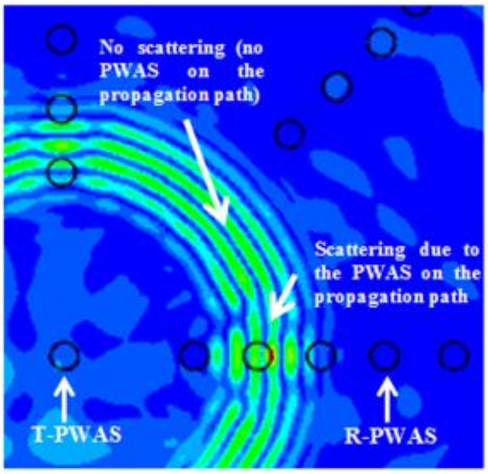


Figure 4. Snapshot of the guided waves propagation showing the scattering due to the bonded PWAS on the guided wave propagation path between the T-PWAS and the R-PWAS (Gresil & Giurgiutiu 2014).

## 3.2 *Electromechanical impedance spectroscopy*

The principles of electromechanical impedance method are illustrated in Figure 5. The drive-point impedance presented by the structure to the active sensor can be expressed as the frequency dependent variable

$$Z_{str}\left(\omega\right)=k_{str}\left(\omega\right)/\,j\omega=k_{e}\left(\omega\right)-\omega_{m}^{2}\left(\omega\right)+j\omega c_{e}\left(\omega\right) \quad (2)$$

Through the mechanical coupling between PWAS and the host structure, on one hand, and through the E/M transduction inside the PWAS, on the other hand, the drive-point structural impedance is reflected directly in the electrical impedance, $Z(\omega)$, at the PWAS terminals

$$Z(\omega)=\left[j\omega c\left(1-\kappa_{31}^{2}\frac{\chi(\omega)}{1+\chi(\omega)}\right)\right]^{-1} \quad (3)$$

where C is the zero-load capacitance of the PWAS and $\kappa_{31}$ is the E/M cross coupling coefficient of the PWAS $\left(\kappa_{31}=d_{31}/\sqrt{s_{11}\bar{\varepsilon}_{33}}\right)$, and $\chi(\omega)=k_{str}/k_{PWAS}$ with $k_{PWAS}$ being the static stiffness of the PWAS.

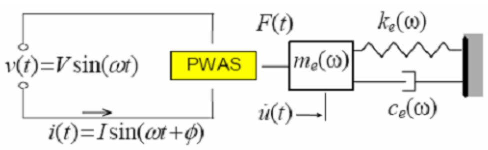


Figure 5. Electromechanical coupling between PWAS and structure for 1-D dynamic model

The electromechanical impedance SHM method is direct and easy to implement, the only required equipment being an electrical impedance analyser, such as the HP 4192A impedance analyser. An example of performing PWAS electromechanical impedance spectroscopy is presented in Figure 6. The HP 4194A impedance analyser (Figure6a) reads the in-situ electromechanical impedance of the PWAS attached to a specimen. It is applied by scanning a predetermined frequency range in the high kHz band (up to 15 MHz) and recording the complex impedance spectrum.

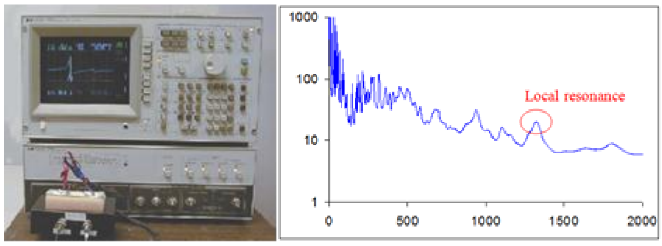


Figure 6. (left) Impedance analyser; (right) example of measured impedance spectrum (Gresil et al. 2012).

During a frequency sweep, the real part of the E/M impedance, $\mathrm{Re}[Z(\omega)]$, follows the up and down variation as the structural impedance goes through the peaks and valleys of the structural resonances and anti-resonances (Figure 6b). By comparing the real part of the impedance spectra taken at various times during the service life of a structure, meaningful information can be extracted pertinent to structural degradation and ongoing damage development. On the other hand, analysis of the impedance spectrum supplies important information about the PWAS integrity. The frequency range used in the E/M impedance method must be high enough for the signal wavelength to be significantly smaller than the defect size. From this point of view, the high frequency EMIS method differs from the low-frequency modal analysis approaches.

In the MP-FEM approach, the mechanical coupling between the structure and the sensor is implemented by specifying boundary conditions of the sensor while the electromechanical coupling is modelled by multi-physics equations for the piezoelectric material. The first coupling allows the mechanical response sensed by the piezoelectric element to be reflected in its electric signature composite. The glass fibre reinforced polymer (GFRP) structure considered in this study is modelled as a homogeneous orthotropic material (Gresil, Yu, Giurgiutiu, & Sutton, 2012). The test specimen is numerically modelled with the MP-FEM method using a 3D mesh. The SOLID186 layered structural solid element is used to model the five layers laminated GFRP composite specimen with layer orientation of 0 degree on the x-axis; the adhesive layer is modelled with the SOLID95 element. The PWAS transducer is modelled with the SOLID226 coupled field element. Each element has twenty nodes. At low frequency (below 500 kHz), at medium frequency (500 kHz to 5 MHz) and at high frequency (5 to 15 MHz), the size of the mesh is 1mm, 0.5mm and 0.1mm respectively, to obtain a good convergence of the problem.

The comparison between the simulated and the experimental impedance spectra results are presented in Figure 7. In Figure 7, the results are in the range up to 5 MHz. It is apparent that a relatively good agreement between the experiments and 3D MP-FEM simulation has been achieved. The good matching is achieved by adjusting the damping coefficients used in the structural model. The correlation of the modal frequencies between the experimental and the numerical results is quite good, especially at higher frequencies. However, some discrepancies in the magnitudes of some resonances are observed, especially in the range of 450 to 650 kHz. It is interesting to see that the best match is obtained in the 700 kHz to 2 MHz frequency range. This is very beneficial, because this frequency range has shown the best detection of delamination damage (Gresil et al., 2012).

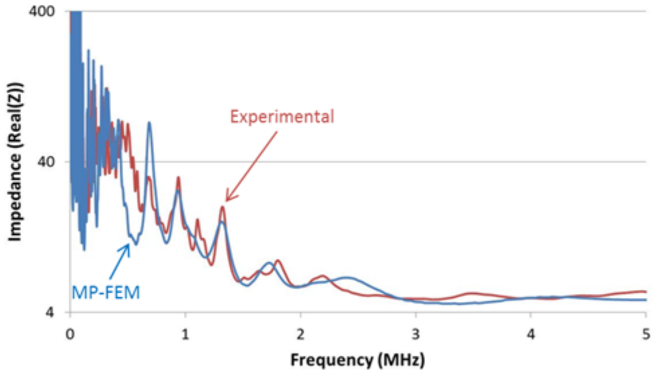


Figure 7. Comparison of experimental and 3D MP-FEM model impedance spectra of laminate GFRP for a frequency range 10 kHz to 5 MHz (Gresil et al. 2012).

Figure 8 shows a comparison of the impedance spectra in a very high frequency range (of 5 to 15 MHz).

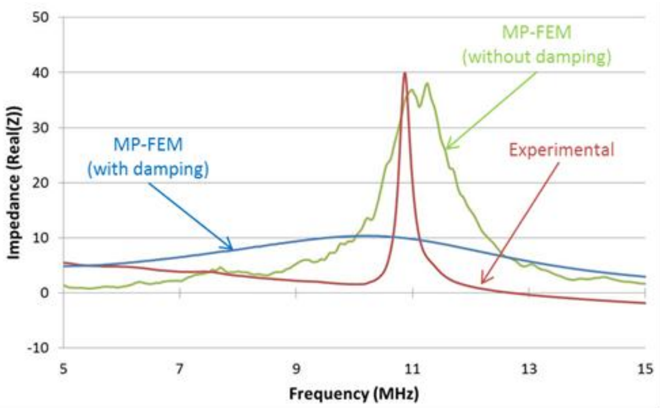


Figure 8. Comparison of experimental and 3D MP-FEM model impedance spectra of laminate GFRP for a frequency range 5 MHz to 15 MHz (Gresil et al. 2012).

Only one peak is observed at ~11 MHz; this peak corresponds to the thickness mode resonance of the PWAS transducer. It seems that at high frequency (5 to 15 MHz), the vibration is localized near the PWAS so the bonding condition and the PWAS geometry is very important. In the case of the simulation the bonding layer is perfect and also the PWAS geometry. In reality, this is not true so we can explain more difference between the experimental and the simulation results for high frequency. Moreover the magnitude of the vibration pick is very small due to the damping effect, and this effect is very hard to simulate because of the non-linearity of this effect. The comparison between the 3D simulation and experimental results has revealed two different regions of behaviour: (i) below 5 MHz, the experimental result matches the result from a 3D model with structural damping (Figure 7); (ii) however, above 7 MHz, the experimental result matches better with a 3D model without structural damping (Figure 8). One possible explanation is that at lower frequency the vibration covers a larger area and the overall structural damping is important; whereas at high frequency the vibration is localized in thickness mode resulting that the structural damping has negligible effect. In comparison with other models of the EMIS technique, the model discussed here exhibits remarkable robustness at very high frequency (Gresil et al., 2012).

## 4 SUMMARY AND GUIDELINES FOR FUTURE WORK

PWAS have been shown to be very well-suited for structural health monitoring. The same set of piezoelectric elements can be utilised for ageing monitoring, damage detection, location and identification, and finally to record the AE activity of the structure under test.

The multi-functional character of PWAS is quite relevant in its application to the on-line health monitoring of aeronautical structures. In practice, the use of the same set of sensors to perform at least three kinds of measurement reduces the weight of the monitoring system and hence simplifies the maintenance process.

Furthermore, it will be of great interest to develop wireless frameworks of sensors allowing both weight savings and simplification of the insertion process, especially in the case of the articulated parts of a complex structure. In conclusion, PWAS have great potential for development in the field of SHM. In the near future, more multi-functional SHM systems have to be developed to collect different kinds of signals and physical parameters with the same network of sensors.

# 5 REFERENCES


ACARE. (2001). *Advisory Council for Aeronautics Research in Europe - European Aeronautics: a vision for 2020*.

Diamanti, K., & Soutis, C. (2010). Structural health monitoring techniques for aircraft composite structures. *Progress in Aerospace Sciences, 46*(8), 342-352.

Giurgiutiu, V. (2008). *Structural Health Monitoring With Piezoelectric Wafer Active Sensor*: Elsevier Academic Press.

Gresil, M., & Giurgiutiu, V. (2013a). *Guided wave propagation in carbon composite laminate using piezoelectric wafer active sensors.* Paper presented at the SPIE Smart Structures and Materials+ Nondestructive Evaluation and Health Monitoring, San-Diego, CA, USA.

Gresil, M., & Giurgiutiu, V. (2013c). *Prediction of attenuated guided wave propagation in carbon fiber composites*. Paper presented at the The 19th International Conference on Composite Materials, Montreal, Canada.

Gresil, M., & Giurgiutiu, V. (2014). Prediction of attenuated guided waves propagation in carbon fiber composites using Rayleigh damping model. *Journal of Intelligent Material Systems and Structures*. doi: 10.1177/1045389x14549870

Gresil, M., Soutis, C., & Giurgiutiu, V. (2014). *Ultrasonic Structural Health Monitoring – An Overview.* Paper presented at the 53rd Annual Conference of The British Institute of Non-Destructive Testing, Manchester, UK.

Gresil, M., Yu, L., Giurgiutiu, V., & Sutton, M. (2012). Predictive modeling of electromechanical impedance spectroscopy for composite materials. *Structural Health Monitoring, 11*(6), 671-683.

Gresil, M., Yu, L., Shen, Y., & Giurgiutiu, V. (2013). Predictive model of fatigue crack detection in thick bridge steel structures with piezoelectric wafer active sensors. *Smart Structures and Systems, 12*(2), 001-635.

Grondel, S., Assaad, J., Delebarre, C., & Moulin, E. (2004). Health monitoring of a composite wingbox structure. *Ultrasonics, 42*(1–9), 819-824.

Haase, P., Thomson, R., Bishop, P., & Isambert, E. (2013). EASA.2011.NP.24 "Composite Damage Metrics and Inspection" (CODAMEIN II) *EASA.2011.NP.24 Report*

Ihn, J.-B., & Chang, F. K. (2008). Pitch-catch active sensing methods in structural health monitoring for aircraft structures. *Structural Health Monitoring, 7*(1), 5-19.

Jong-In, K., Hyung-Joon, B., Chun-Gon, K., & Chang-Sun, H. (2005). Simultaneous measurement of strain and damage signal of composite structures using a fiber Bragg grating sensor. *Smart Materials and Structures, 14*(4), 658.

Koh, Y. L., Chiu, W. K., Rajic, N., & Galea, S. C. (2003). Detection of Disbond Growth in a Cyclically Loaded Bonded Composite Repair Patch Using Surface-mounted Piezoceramic Elements. *Structural Health Monitoring, 2*(4), 327-339.

Martin, T., Hudd, J., Wells, P., Tunnicliffe, D., & Das-Gupta, D. (2001). The Use of Low Profile Piezoelectric Sensors for Impact and Acoustic Emission (AE) Detection in CFRC Structures. *Journal of Intelligent Material Systems and Structures, 12*(8), 537-544.

Perez, I. M., Cui, H., & Udd, E. (2001). *Acoustic emission detection using fiber Bragg gratings*.

Pfeiffer, H., & Wevers, M. (2007). *Aircraft Integrated Structural Health Assessment – Structural Health Monitoring and its implementation within the European project AISHA*. Paper presented at the EU Project Meeting on Aircraft Integrated Structural Health Assessment (AISHA), Leuven, Belgium.

Staszewski, W. J., Mahzan, S., & Traynor, R. (2009). Health monitoring of aerospace composite structures – Active and passive approach. *Composites Science and Technology, 69*(11–12), 1678-1685.

Sung, D.-U., Oh, J.-H., Kim, C.-G., & Hong, C.-S. (2000). Impact Monitoring of Smart Composite Laminates Using Neural Network and Wavelet Analysis. *Journal of Intelligent Material Systems and Structures, 11*(3), 180-190.